Sensors and Actuators B 254 (2018) 519–525

Contents lists available at ScienceDirect

Sensors and Actuators B: Chemical

journal homepage: www.elsevier.com/locate/snb

Thermally induced reversible and reprogrammable actuation of tough hydrogels utilising ionoprinting and iron coordination chemistry

Anna B. Baker[a,b,*], Duncan F. Wass[c], Richard S. Trask[a]

[a] Department of Mechanical Engineering, University of Bath, Bath, BA2 7AY, UK
[b] Advanced Composite Centre for Innovation and Science (ACCIS), Department of Aerospace Engineering, University of Bristol, Bristol, BS8 1TR, UK
[c] School of Chemistry, University of Bristol, University of Bristol, Bristol, BS8 1TS, UK

ARTICLE INFO

Article history:
Received 20 April 2017
Received in revised form 3 July 2017
Accepted 14 July 2017
Available online 17 July 2017

Keywords:
Ionoprinting
Hydrogel
Interpenetrating polymer network
Actuation
Temperature responsive

ABSTRACT

Ionoprinting has proven itself as a technique capable of enabling repeated post-synthesis programming of hydrogels into a variety of different shapes, achieved through a variety of different actuation pathways. To date, the technique of ionoprinting has been limited to conventional brittle hydrogels, with reversible actuation requiring a change in submersion solution. In this study, ionoprinting has been combined for the first time with a tougher interpenetrating network polymer (IPN) hydrogel with dual pH and temperature responsiveness. This new methodology eliminates the brittle material failure typically occurring during shape change programming and actuation in hydrogels, thus allowing for the realisation of more highly strained and complex shape formation than previously demonstrated. Critically, the temperature responsiveness of this system enables actuation between an unfolded (2D) and a folded (3D) shape through an external stimuli; enabling reversible actuation without a change in submersion solution. Here, the reversible thermally induced actuation is demonstrated for the first time through the formation of complex multi-folded architectures, including an origami crane bird and Miura folds, from flat hydrogel sheets. The robustness of the IPN hydrogel is demonstrated through multiple reprogramming cycles and repeated actuation of a single hydrogel sheet formed into 3D shapes (hexagon, helix and zig-zag). These advancements vastly improve the applicability of ionoprinting extending its application into areas of soft robotics, biomedical engineering and enviro intelligent sensors.

1. Introduction

Hydrogels are three-dimensional polymer networks which are able to absorb large amounts of water [1]. They have current and potential uses in biomedical, agricultural and waste treatments applications [2]. Hydrogels often possess comparable mechanical properties to biological tissue, but with significantly reduced toughness [3]. A number of approaches have been shown to significantly increase the toughness of these materials, the most widely demonstrated has been the utilisation of multiple polymer networks [3,4]. Such additional polymer networks may involve covalent crosslinking (double, triple etc. network hydrogels), ionic crosslinking (ionic-covalent network (ICE) hydrogels) or secondary bonds (interpenetrating polymer network (IPN) hydrogels) [4].

Depending on their molecular composition, hydrogels can also show stimuli-responsiveness to a range of stimuli including light, pH and temperature, undergoing large volume changes in response [5]. Stimuli-responsive hydrogels have the potential to be used in sensing, actuating and drug delivery applications [6–8]. The ability to induce shape change, not simple volume change, further extends the application of stimuli responsive hydrogels [9]. Single composition hydrogel i.e. homogenous hydrogels, will only undergo inhomogeneous volume change i.e. shape change, when exposed to inhomogeneous stimuli [10]. For a hydrogel to undergo shape change in response to a uniform (homogenous) stimuli, the introduction of an embedded inhomogeneity is required. This has conventionally been achieved during the synthesis/manufacture of the hydrogel through the use of bilayers, aligned reinforcements and spatially variable crosslinking [11–18]. Ionoprinting introduces inhomogeneity into a hydrogel after synthesis, by ionically crosslinking localised regions of the hydrogels [19–26]. The increasing ionic crosslinking causes a reduction in hydrogel water content and thus volume, while increasing hydrogel stiffness; which when localised to specific areas of the hydrogel can cause inhomogeneous

* Corresponding author at: Department of Mechanical Engineering, University of Bath, Bath, BA2 7AY, UK.
E-mail address: a.b.baker@bath.ac.uk (A.B. Baker).

http://dx.doi.org/10.1016/j.snb.2017.07.095

shape change. Ionoprinting achieves this localised ionic crosslinking by surface injection of metal cations, which are generated in situ via an oxidative bias generated by an electric field. The dynamic nature of the ionic crosslinks allows them to be formed after manufacturing through the introduction of metal cations and destroyed on demand by removal of the metal cations through a competing coordinating species. This dynamic nature allows for post-synthesis shape change programming and subsequent removal of the cations, returning the hydrogel to its originally synthesised state, allowing for new re-programming of further shape changes. However, the shape changes demonstrated to date have been very limited and simplistic, which is believed to be due to the inability to create complex reversible shape changes derived from brittle hydrogels (due to material failure during ionoprinting and actuating conditions).

In this study, a dual pH-temperature responsive interpenetrating polymer network hydrogel is programmed to undergo reversible shape change and actuation through ionoprinting of hinges. This work explores the factors controlling the hinge formation through an investigative study of the ionoprinting input variables and the conductivity of the hydrogel. A variety of thermally induced reversible shape changes are then demonstrated, all showing 2D (hot) to 3D (cold) transformations.

2. Materials and methods

2.1. Materials

N-isopropylacrylamide (NIPAAm), phosphoric acid 2-hydroxyethyl methacrylate ester (PHMA), *N*,*N*′-methylenebisacrylamide (MBAA), 2,2-dimethoxy-2-phenylacetophenone (DMPA), Lithium chloride (LiCl), iron(III) chloride hexahydrate, disodium ethylenediaminetetraacetic acid (EDTA) and triethylamine (TEA) were obtained from Sigma-Aldrich (Poole, UK). 2-(methacryloyloxy)ethyl phosphate (MOEP) was extracted from PHMA with n-hexane, all other chemicals were used as supplied without further purification. Polyurethane (PU HydroMed D3) was supplied by AdvanSource biomaterials and was used as a 10% w/v solution in reagent grade ethanol.

2.2. Hydrogel synthesis

IPN hydrogels were prepared by combining the monomers (NIPAAm and MOEP, 80:20 molar ratio) followed by neutralisation with TEA. This mixture (40.0% weight) was dissolved in PU solution prior to the addition of the photoinitiator (DMPA, 1:750 photoinitiator:monomer molar ratio) and the crosslinker (DMPA, 1:500 crosslinker:monomer molar ratio). For single network (SN) hydrogels the same procedure was followed however monomer mixtures were dissolved in ethanol instead of PU stock solution. All the solutions were cured in either 1 ml syringes (internal diameter of 5 mm) or between two glass slides separated by a spacer (1.0 mm thickness). Samples were cured under a UV lamp (365/425 nm, 4 W) for 4 h. Hydrogels were submerged into DI water after curing to precipitate the PU out of solution to form the second interpenetrating network. Pure hydrogel samples were air dried prior to submersion into water to prevent brittle failure.

2.3. Ionoprinting & actuating conditions

Prior to ionoprinting hydrogel samples were equilibrated in 0.1 M LiCl solution, unless otherwise stated, for a minimum of 48 h. Immediately prior to ionoprinting the hydrogels were removed from their equilibration solution and pat dried. Ionoprinting was performed using an iron wire anode (diameter 2.8 mm) and a flat aluminium sheet (surface area greater than the hydrogel) with pressure onto the hydrogel controlled by a spacer (thickness 1.0 mm). The variables tested ranged from 0.5 to 5.0 min for duration, 2.0–10.0 V for input voltage and 0.05–1.00 M for LiCl solutions. The standard baseline conditions used throughout this study were 5.0 V for 1 min for ionoprinting of a hydrogel swollen in 0.1 M LiCl solution. Samples used to investigate ionoprinting variables were 20 mm by 5 mm by 0.6 mm (water swollen dimensions) hydrogels. The voltage measured through the entire system was assumed to be the voltage occurring through the hydrogel (i.e. the only significant resistive element in the circuit), whilst the current was measured in series (range up to 200 mA with an accuracy of 0.1 mA or a range up to 5.00 A with an accuracy of 0.01 A) recorded every 5 s and integrated to determine moles of electrons through the circuit. Final out-plane-angle was measured immediately after ionoprinting and were repeated 3 times.

Actuation was performed in the equilibration solution, samples were heated to 50 °C (for 1 h) to enable unfolding of the ionoprinted hinges and cooled to 25 °C (for 1 h) to enable folding of the ionoprinted hinges. Cations were extracted with EDTA overnight and re-equilibrated in 0.1 M LiCl solution before further ionoprinting.

2.4. Hydrogel characterisation

The hydrogel's response to a range of environmental stimuli was investigated by submersion for 24 h in different solutions, including various concentrations of iron(III) chloride (0.0 M–5.0 M) and buffer solutions (0.1 M NaCl and 0.01 M buffer) over a range of temperatures (10–90 °C).

Compressive testing was performed between two parallel plates on disc samples, diameter 7.0 mm (0.1 mm standard deviation (STD) by 3.7 mm (0.6 mm STD) thickness for SN hydrogels and diameter 7.6 mm (0.1 mm STD) by 4.1 mm (0.6 mm STD) thickness for IPN hydrogels) at a rate of 100% min^{-1} until failure. Compressive modulus (up to 20% strain), energy absorbed until failure and stress and strain at failure were determined.

3. Results and discussion

3.1. Ionoprinting fundamentals

The process of ionoprinting employs an oxidative bias generated by an electric field to produce metal cations, these are utilised for ionic crosslinking within a hydrogel [19]. For the hydrogel to be successfully ionically crosslinked by the cations, coordinating groups must be present within the hydrogel. The ionic bridging of these coordination groups triggers the explosion of the water molecules leading to the shrinking of the hydrogel. Throughout this study a flat aluminium sheet was employed as the cathode whilst an iron wire was used as the anode, as shown in Fig. 1a. When a potential is applied across the system a number of simultaneous electrochemical processes are established; at the anode the oxidation of the iron metal to iron(III) cations (Fe^{3+}) and at the cathode the reduction of protons to hydrogen. While the metal cations become bound within the hydrogel, forming the ionic crosslinks, the hydrogen gas leaves the system.

The ionic crosslinking is locally concentrated near the anode-hydrogel interface, with the concentration decreasing with increasing distance from this interface. The ionic crosslinking results in localised shrinking of the hydrogel (see supplementary Fig. S1), while leaving the remaining hydrogel swollen, the internal stresses generated by this swelling differential is relieved through the out-of-plan folding of hydrogel along the ionoprinted line, as shown in Fig. 1b. The ionoprinted hinge can be unfolded back to the original configuration by de-swelling the non-ionoprinted regions of the hydrogel, i.e. removing the differential in swelling within the specimen, by heating the hydrogel above its lower critical solution

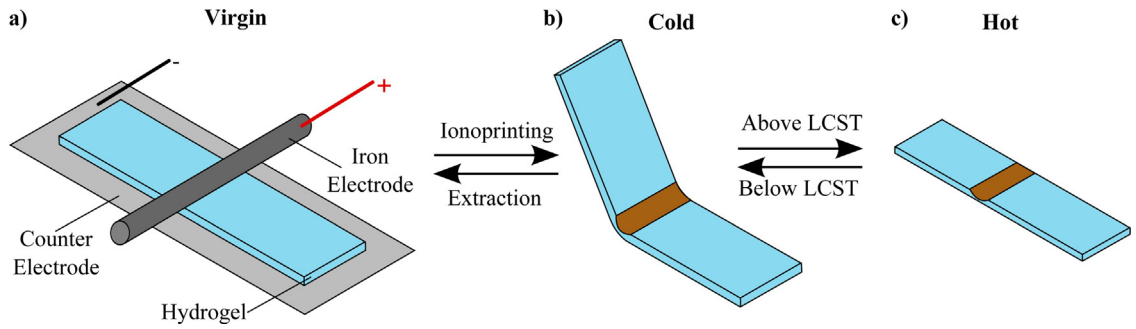

Fig. 1. Schematic diagram of ionoprinting of a hydrogel with iron cations. a) Ionoprinting using an iron electrode (anode) and aluminium counter electrode (cathode). b) & c) Ionoprinted hydrogel folded and unfolded, oscillating between below LCST and above LCST, respectively.

temperature (LCST), as shown in Fig. 1c, and refolded by cooling the hydrogel below its LCST; where refolding will occur due to the reestablishment of the swelling differential between ionoprinted and non-ionoprinted regions.

3.2. Actuation variables

Previously, a number of ionoprinting variables have been investigated including voltage, electrode composition and the concentration of coordinating groups, dimensions and pH of the hydrogel, determining their effect on amount of cations produced and curvature induced [19–21,23,25]. Here, both the voltage and duration of ionoprinting process are investigated along with the variation in conductivity of the hydrogel's pre-ionoprinting equilibration solutions.

Increasing or decreasing either the voltage or duration of ionoprinting had the same effect on both the out-of-plane angle and the total amount of electrons produced through ionoprinting, as shown in Fig. 2a and b. These trends are attributed to either increased voltage resulting in an increase in current through the hydrogel and therefore a greater amount of cations generated and a greater out-of-plane deflection, or a longer printing time resulting in more cations generated and again a greater out-of-plane deflection. However, the rate of increase decreased with increased voltage or duration, i.e. per volt or per minute, which is attributed to the build up of cations in the hydrogel near the anode increasing the resistance of the hydrogel thereby decreasing the current through the hydrogel as ionoprinting progresses; resulting in a decreased rate of cation production and out-of-plane deflection.

The conductivity of the swollen hydrogel can be altered by changing the conductivity of the solution in which it is equilibrated within. For example, LiCl had a minimal effect on swelling of the hydrogel, yet it is capable of significantly altering its resistance, i.e. the stronger the concentrations of LiCl solution the lower the resistance of the hydrogel [27]. This reduction in resistance with increasing hydrogel conductivity can be seen in Fig. 2c, through the increase in electrons flow through the ionoprinting process. However, it should be noted, that the increase in transferred electrons does not positively correlate to out-of-plane angle generated at the fold. It is hypnotised that this is due to an increase in a competing redox reaction, indicated by a change in the ratio of visible products, i.e. an increase in colourless bubble formation at the aluminium cathode-hydrogel interface and the simultaneous reduction in visible colourisation around the anode-hydrogel interface (i.e. Fe^{3+}). Within the system other species could undergo oxidation instead of the iron including chloride (Cl^{-1}) and hydroxide ions (OH^{-1}); the oxidation of either of these species would not be visibly observable in the current system as both form gaseous products at the exposed interface. This observed reduction in Fe^{3+} cations results in a reduction in the number of ionic crosslinks formed within the

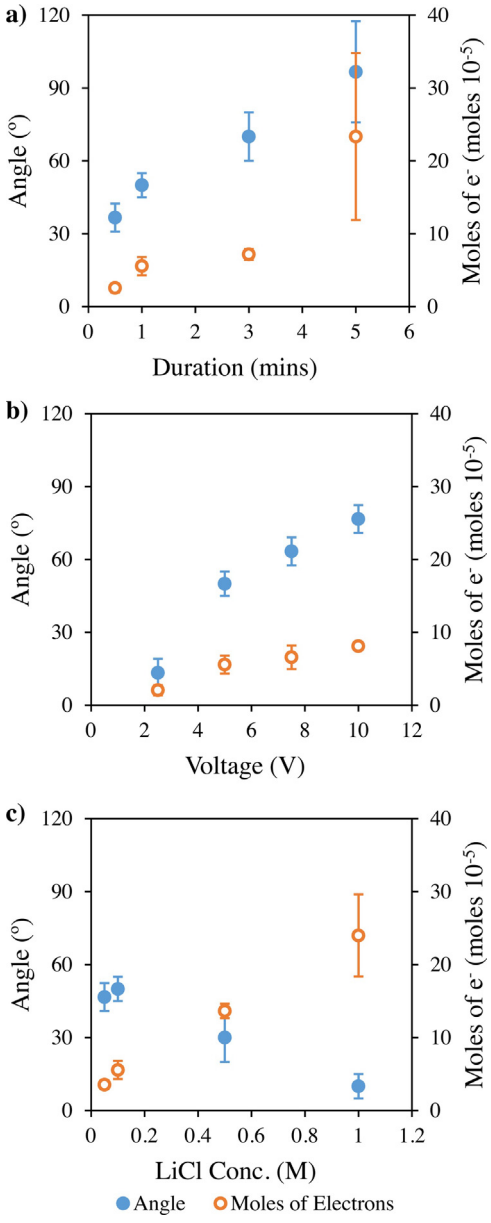

Fig. 2. The out-of-plane final angle formed (filled marker, to the nearest 10°) and moles of electrons produce due to ionoprinting (open marker) at **a)** variable durations (30 s–5 min), **b)** variation voltages (2.5–10.0 V) and **c)** variable LiCl equilibration solution concentrations (0.05–1.00 M). Standard conditions ionoprinted 1 min at 5 V equilibrated in 0.1 M LiCl solution. Data point mean average of 3 repeats (error bar = ±1 standard deviation).

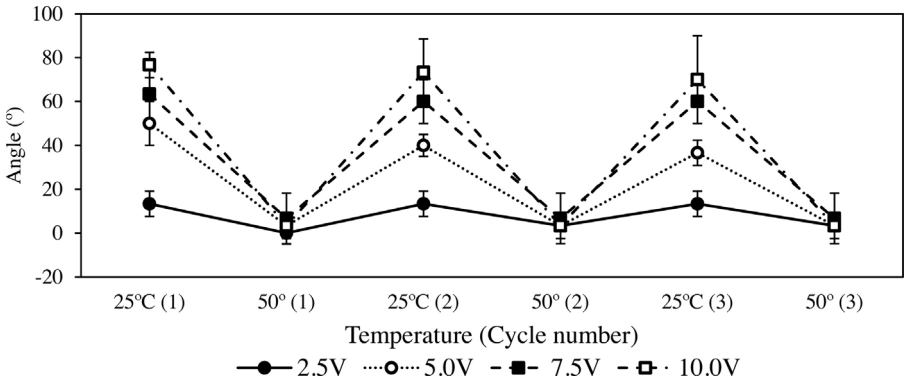

Fig. 3. The out-of-plane angle formed at various voltages (2.5 V–10.0 V) at 25 °C and 50 °C through 3 cycles. Data point mean average of 3 repeats (error bar = ±1 standard deviation).

hydrogel and the shrinkage of the ionoprinted region, causing a smaller out-of-plane deflection. It is through the correct control and balance of these key variables that out-of-plane reversible actuation can be used to create shape change materials with controlled and predictable hinge formation.

The reversible actuation of the hinge was investigated at various ionoprinting voltages by cycling the hydrogel between 25 °C and 50 °C for three cycles, see Fig. 3. The hydrogel hinges were capable of unfolding and refolding through heating and cooling without a change in submersion solution. The hydrogels showed no visible signs of failure during this cycling, a behaviour not observed with the SN hydrogels, which showed cracking or complete failure during cycling (see supplementary Fig. S5).

3.3. Reversible actuation

The ability to form 3D shapes from 2D planar hydrogels is demonstrated here through the formation of a variety of predictable, programmable and reversible shape changes. Like many other polymeric based actuating systems, the technique of ionoprinting has been demonstrated by the formation of cubes from a flat cruciform hydrogel, for example as shown in Fig. 4 for the current system. The formation of the cube was demonstrated by ionoprinting 5 hinges onto the virgin cruciform hydrogel (Fig. 4a) with all hinges demonstrating an out-of-plane deformation of 90° (Fig. 4c). The reversible actuation of this cube was demonstrated by heating the hydrogel in its equilibration solution (0.1 M LiCl) to 50 °C resulting in the complete unfolding of the hydrogel back into its cruciform shape. However, as the actuation is a result of the deswelling of the non-ionoprinted hydrogel the original size is not restored (Fig. 4b). The reversible actuation from cube (cold) and flat cruciform (hot) can be achieved by simply cycling the hydrogel below and above its LCST, respectively. The LCST of the hydrogel in 0.1 M LiCl solution is 37 °C. The temperature of the LCST can be shifted by variation in pH, with the hydrogel showing interlinked pH and temperature volume change (see supplementary information Fig. S2). The majority of ionoprinting reported previously only induced actuation by changing the sample submersion solution, here an external stimuli has been utilised to achieve reversible actuation instead.

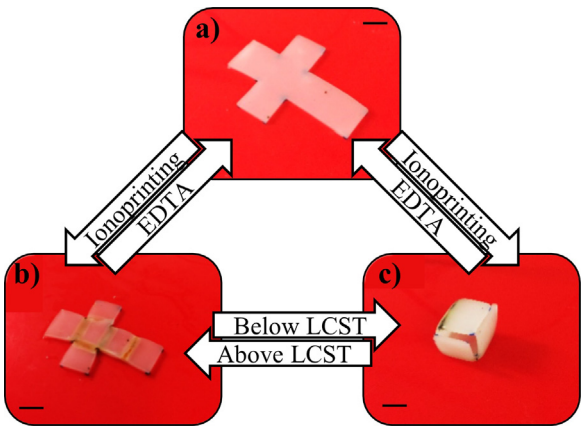

Fig. 4. Reversible actuation of a cube, formed from a flat cruciform hydrogel **(a)** through ionoprinting four 90° hinges to form a 3D cube **(c)**, capable of unfolding through heating above the LCST of the hydrogel **(b)** and refolding by cooling below the LCST of the hydrogel **(c)** Scale bar = 5 mm.

Due to the nature of the ionic crosslinks formed within the hydrogel, the crosslinking can be destroyed by removing the cations; this does not occur through diffusion alone but can be achieved through the use of a chelating agent (see supplementary information Fig. S3). In this study, ethylenediaminetetraacetic acid (EDTA) is used to remove the cations through the formation of a Fe^{3+}-EDTA complex, which breaks down the ionic crosslinks and restores the hydrogel back to a virgin state. This hydrogel can then be re-ionoprinted into the same shape changing system or into a completely different configuration. This ability for reprogramming is explored in Section 3.4.

The brittle nature of most hydrogels has restricted their potential to act as shape changing architectures achievable through ionoprinting. The introduction of a secondary PU network significantly enhances the toughness of the hydrogel along with other mechanical properties (see supplementary information Table S1). The technique of ionoprinting relies on internal swelling and stiffness differentials to achieve actuation. However, it is the magnitude of this differential which triggers stress induced cracking throughout the hydrogel both during the ionoprinting process and the cyclic actuation (see supplementary Figs. S4). The use of a tougher IPN hydrogel allows for more highly strained and complex shape change formations, thus permitting large out-of-plane deformation and multi and interconnected hinges, along with repeatable cyclic actuation never previously demonstrated. For example, here we demonstrate the formation of (1) an origami crane bird from an irregular 4 pointed star and (2) a series of Miura folds formed from a flat 2D rectangle hydrogels, as shown in Figs. 5 and 6. Both shape changes rely on the formation of intersecting mountain and valley folds; these architectures are frequently employed in many origami designs and therefore the ability to achieve these fold-combinations is essential for the realisation of complex morphing. The intersecting hinges are formed with mountain and valley folds on opposite surfaces of the hydrogel, therefore hinges of opposite nature never interact with each other and the opposing stress they cause can be distributed through the thickness of the hydrogel.

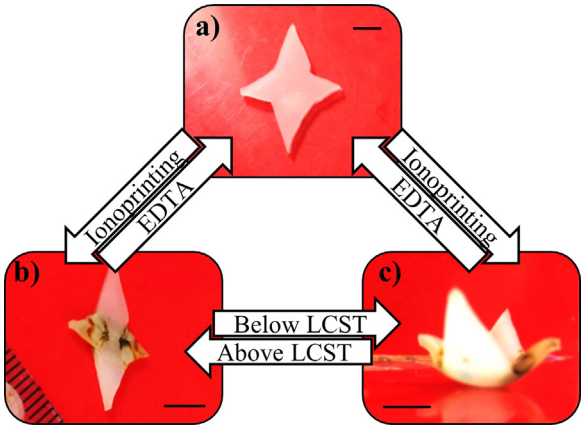

Fig. 5. Reversible actuation of an origami crane bird, formed from a flat four pointed irregular star **(a)** through ionoprinting 7 valley and 2 mountain folds (see supplementary information Fig. S5) **(c)**, capable of unfolding through heating above the LCST of the hydrogel **(b)** and refolding by cooling below the LCST of the hydrogel **(c)** Scale bar = 5 mm.

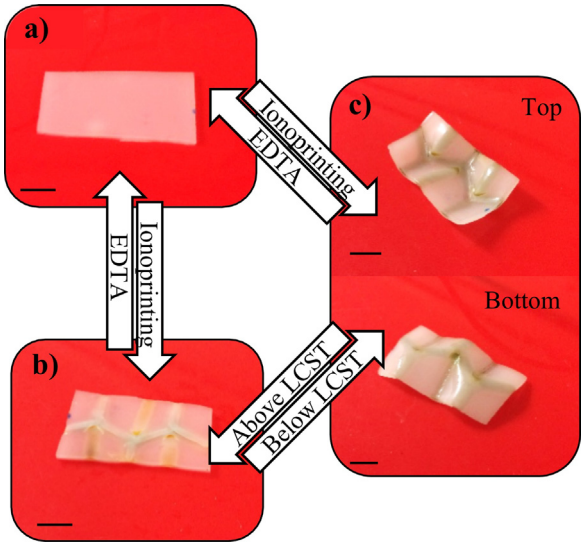

Fig. 6. Reversible actuation of a series of Miura folds, formed from a flat rectangular hydrogel **(a)** through ionoprinting 7 valley folds and 3 mountain folds (see supplementary information Fig. S5), top and bottom view of out-of-plane deformation **(c)**, capable of unfolding by heating above the LCST of the hydrogel **(b)** and refolding by cooling to below the LCST of the hydrogel **(c)** Scale bar = 5 mm.

Both shape changes use 4-fold vertices formed from 3 folds of one type and 1 of the opposite type, i.e. 3 mountain folds and 1 valley or 3 valley folds and 1 mountain. The angles formed by each hinge in the arrangement is described by J. Na et al. and depicted in Fig. 7 [28]; this comprises of one mountain and one valley fold interesting at the vertex from exactly opposite directions with the same magnitude in out-of-plane deflection ($\theta_1 = -\theta_3$). The remaining two folds are of the same nature (either 2 mountain or 2 valley folds), intersecting at the vertex at equal angles away from the other folds, i.e. they are mirrors of each other with the mirror plane being the pair of mountain and valley fold. Finally, it should be noted that these folds are formed from an equal magnitude of out-of-plane deformation ($\theta_2 = \theta_4$) with the relationship determined by the angle between the unique fold type and the mirrored pair of folds (i.e. S in Fig. 7).

The ionoprinting of the Miura folds used an S angle of 65°, with θ_1 and θ_3 printed to an out-of-plane angle of 45° and θ_3 and θ_2 to angle of 90°. These out-of-plane fold angles were achieved through varying the ionoprinting duration (i.e. printing at 5 V with

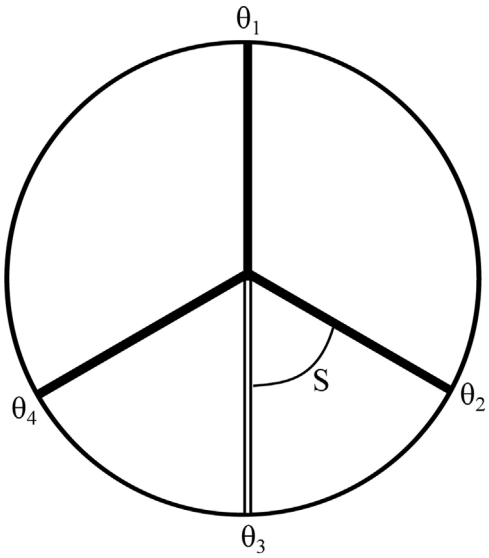

Fig. 7. Diagram of 4-fold vertex found within the crane origami bird and Miura fold patterns. Formed from 3 mountain or valley folds (black lines) and 1 valley or mountain fold (white lines). Equation to determine out-of-plane fold angle. Where angle between θ_1 and θ_3 is 180° and the angle between θ_3 and θ_2 is equal to the angle between θ_3 and θ_4 [28].

a submersion solution of 0.1 M LiCl). The printing time required to achieve these fold angles was determined using Fig. 2a, printing times 45 s and 4 min were required to achieve the angles of 45° and 90°, respectively.

The ionoprinting process requires the sequential formation of each hinge (see supplementary information Fig. S5 for hinge printing order), which results in the partial formation of the folded shape during the printing process. To print the remaining hinges often requires the flattening of the 3D hydrogel to enable full contact with the flat aluminium cathode. This is only achievable due to the tough nature of the IPN hydrogel material.

As before the 3D shapes (Fig. 5 c and 6 c) could be returned to their planar forms through heating to above the LCST of the hydrogel (50 °C) as shown in Figs. 5 b and 6 b and returned to their folded shape through cooling below the LCST (25 °C). The virgin hydrogel can be successful restored through the use of the chelating agent EDTA, as shown in Figs. 5 a and 6 a.

3.4. Reprogramming multiple shape actuation

The actuation pathways demonstrated have shown reversible transformation between 2 shape and 3 state actuation through cycling the hydrogels between a thermal and ionic crosslinking gradient. Applying these principles, it is possible to transform a single planar rectangular hydrogel into three different 3D shapes. The shape changes demonstrated all utilise ionoprinted hinges of 60° and achieve a variety of different shape changes through variations in the position of these hinges. Three specific configurations were selected to demonstrate reprogrammable shape changes from the same base architecture, i.e. coiling, twisting and zig-zagging motions as shown indicated in Fig. 8.

The ability to program a variety of different shape changes demonstrates the post-synthesis nature of the actuation programming, enabling homogenous hydrogels to be programmed to shape change in response to a homogenous stimuli. This approach enables a considerable variety of shape changes to be programmed from a single starting material. In this study, even within the restriction

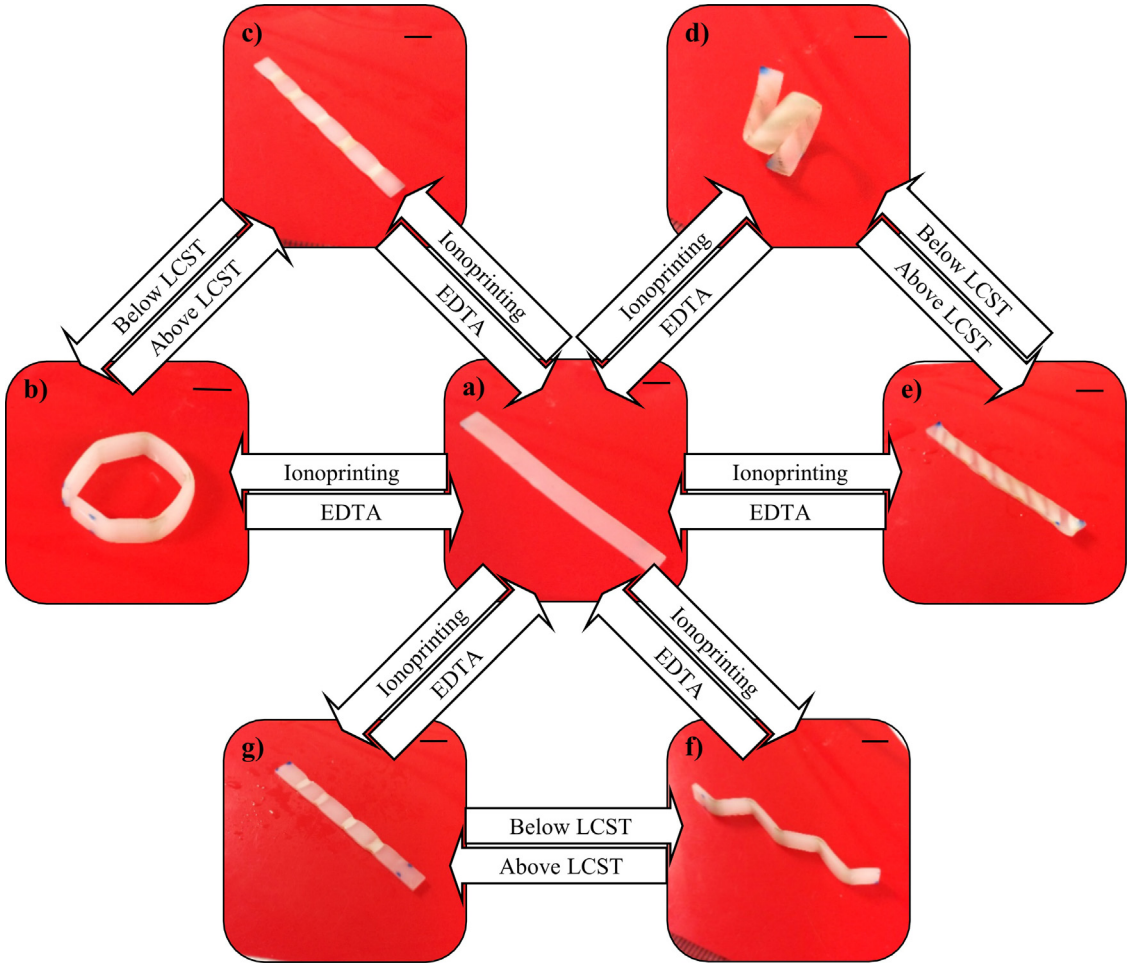

Fig. 8. Multi-shape reversible actuation formed from a flat hydrogel bar **(a)** ionoprinted into a hexagon **(b)**, a coil **(d)** and a zig-zag **(f)** through various ionoprinting patterns (see supplementary information Fig. S5), capable of unfolding to flat rectangular forms while retaining their ionoprinted lines through heating to above the LCST of the hydrogel **(c)**, **(e)** and **(g)** and refolding to reform their hexagon **(b)**, coil **(d)** and zig-zag **(f)** shapes, respectively. Scale bar = 5 mm.

of equal out-of-plane deformation for each hinge and only the use of parallel hinges, three significantly different shape change are demonstrated. The three different shape changes all exhibit the same shape above LCST, i.e. a shrunken planar rectangle (Fig. 8c, e and g), but remember and return to their previous shape below LCST due to the retention of their ionoprinted hinges.

One distinct advantage of this system, and unlike many polymeric based actuators, is the programming is reversible allowing the designer to introduce and switch between new actuation pathways. While in theory, the cyclic actuation and re-programming is achievable with conventional SN hydrogel it has not been demonstrated as conventional SN hydrogels do not possess the robustness required to withstand the cycling and re-programming process. The new IPN hydrogel has overcome this limitation thereby vastly improving the applicability of ionoprinting and extending its use into areas of soft robotics, biomedical engineering and enviro intelligent sensors.

4. Conclusion

This study has shown that the process of ionoprinting can be used as a post-synthesis technique for the programming of a homogenous hydrogel into a variety of complex shape changes. We have developed a stimuli-responsive hydrogel for reversible actuation exhibiting dual pH and temperature responsiveness. The reversible actuation of ionoprinted hydrogels was controlled through the cycling above and below the LCST of the hydrogel, removing the requirement for a change in submersion solution composition (the traditionally preferred method for such systems). The dynamic nature of the ionic crosslinks formed through ionoprinting enable it to be used as a technique that allows multiple re-programming of a single hydrogel into a variety of different shape changes, via deposition, removal and re-deposition of cations species.

Our study has examined the key variables effecting the ionoprinting process indicating how the out-of-plane deformation can be precisely controlled through variations in the voltage and duration of ionoprinting, as well as the conductivity of the hydrogel. These parameters govern the flow of electrons through the system and the out-of-plane angle formed. However, it was noted that the localised build up of cations within the hydrogel increases its resistance thus requiring an increase in voltage and duration to form steeper angles. Conversely, an increase in conductivity of the hydrogel caused greater electron flow through the system but a decrease in out-of-plane angle formed. These variables can be used to achieve predictable, repeatable and programmable reversible actuation of IPN hydrogels. The use of an IPN hydrogel with increased toughness critically overcomes a key failing of current hydrogels (namely the issue of brittle failure), enabling (1) more complex and highly strained shape changes to be demonstrated, (2) the cyclic actuation between 2D and 3D shapes, and (3) the repeated re-programming of a single hydrogel sample into

different complex architectures. These advancements vastly improve the applicability of hydrogel ionoprinting for application in the growth areas of soft robotics, biomedical engineering and enviro intelligent sensors.

Funding

This work was supported by the Engineering and Physical Sciences Research Council through the EPSRC Centre for Doctoral Training in Advanced Composites for Innovation and Science (grant number EP/G036772/1) and RST's EPSRC Engineering Fellowships for Growth (grant number EP/M002489/1).

Appendix A. Supplementary data

Supplementary data associated with this article can be found, in the online version, at http://dx.doi.org/10.1016/j.snb.2017.07.095.

References

[1] W.R.K. Illeperuma, J.-Y. Sun, Z. Suo, J.J. Vlassak, Force and stroke of a hydrogel actuator, Soft Matter 9 (2013) 8504, http://dx.doi.org/10.1039/c3sm51617b.
[2] Q. Chen, H. Chen, L. Zhu, J. Zheng, Fundamentals of double network hydrogels, J. Mater. Chem. B 3 (2015) 3654–3676, http://dx.doi.org/10.1039/C5TB00123D.
[3] S. Naficy, H.R. Brown, J.M. Razal, G.M. Spinks, P.G. Whitten, Progress toward robust polymer hydrogels, Aust. J. Chem. 64 (2011) 1007, http://dx.doi.org/10.1071/CH11156.
[4] C.W. Peak, J.J. Wilker, G. Schmidt, A review on tough and sticky hydrogels, Colloid Polym. Sci. 291 (2013) 2031–2047, http://dx.doi.org/10.1007/s00396-013-3021-y.
[5] N.A. Peppas, P. Bures, W. Leobandung, H. Ichikawa, Hydrogels in pharmaceutical formulations, Eur. J. Pharm. Biopharm. 50 (2000) 27–46, http://dx.doi.org/10.1016/S0939-6411(00)00090-4.
[6] H.J. van der Linden, S. Herber, W. Olthuis, P. Bergveld, Stimulus-sensitive hydrogels and their applications in chemical (micro)analysis, Analyst 128 (2003) 325–331, http://dx.doi.org/10.1039/b210140h.
[7] L. Ionov, Hydrogel-based actuators: possibilities and limitations, Mater. Today 17 (2014) 494–503, http://dx.doi.org/10.1016/j.mattod.2014.07.002.
[8] Y. Qiu, K. Park, Environment-sensitive hydrogels for drug delivery, Adv. Drug Deliv. Rev. 64 (2012) 49–60, http://dx.doi.org/10.1016/j.addr.2012.09.024.
[9] R. Geryak, V.V. Tsukruk, Reconfigurable and actuating structures from soft materials, Soft Matter 10 (2014) 1246–1263, http://dx.doi.org/10.1039/c3sm51768c.
[10] L. Ionov, Polymeric actuators, Langmuir 31 (2015) 5015–5024, http://dx.doi.org/10.1021/la503407z.
[11] Z. Hu, X. Zhang, Y. Li, Synthesis and application of modulated polymer gels, Science 269 (1995) 525–527, http://dx.doi.org/10.1126/science.269.5223.525.
[12] S. Zakharchenko, N. Puretskiy, G. Stoychev, M. Stamm, L. Ionov, Temperature controlled encapsulation and release using partially biodegradable thermo-magneto-sensitive self-rolling tubes, Soft Matter 6 (2010) 2633, http://dx.doi.org/10.1039/c0sm00088d.
[13] G. Stoychev, S. Zakharchenko, S. Turcaud, J.W.C. Dunlop, L. Ionov, Shape-programmed folding of stimuli-responsive polymer bilayers, ACS Nano 6 (2012) 3925–3934, http://dx.doi.org/10.1021/nn300079f.
[14] D. Morales, B. Bharti, M.D. Dickey, O.D. Velev, Bending of responsive hydrogel sheets guided by field-assembled microparticle endoskeleton structures, Small 12 (2016) 2283–2290, http://dx.doi.org/10.1002/smll.201600037.
[15] R.M. Erb, J.S. Sander, R. Grisch, A.R. Studart, Self-shaping composites with programmable bioinspired microstructures, Nat. Commun. 4 (2013) 1712, http://dx.doi.org/10.1038/ncomms2666.
[16] A. Sydney Gladman, E.A. Matsumoto, R.G. Nuzzo, L. Mahadevan, J.A. Lewis, Biomimetic 4D printing, Nat. Mater. 15 (2016) 413–418, http://dx.doi.org/10.1038/nmat4544.
[17] J. Kim, J. Hanna a, M. Byun, C.D. Santangelo, R.C. Hayward, Designing responsive buckled surfaces by halftone gel lithography, Science (80) 335 (2012) 1201–1205, http://dx.doi.org/10.1126/science.1215309.
[18] Y. Zhang, L. Ionov, Reversibly cross-linkable thermoresponsive self-folding hydrogel films, Langmuir 31 (2015) 4552–4557, http://dx.doi.org/10.1021/acs.langmuir.5b00277.
[19] E. Palleau, D. Morales, M.D. Dickey, O.D. Velev, Reversible patterning and actuation of hydrogels by electrically assisted ionoprinting, Nat. Commun. 4 (2013) 2257, http://dx.doi.org/10.1038/ncomms3257.
[20] B.P. Lee, S. Konst, Novel hydrogel actuator inspired by reversible mussel adhesive protein chemistry, Adv. Mater. 26 (2014) 3415–3419, http://dx.doi.org/10.1002/adma.201306137.
[21] B.P. Lee, A. Narkar, R. Wilharm, Effect of metal ion type on the movement of hydrogel actuator based on catechol-metal ion coordination chemistry, Sens. Actuators B Chem. 227 (2016) 248–254, http://dx.doi.org/10.1016/j.snb.2015.12.038.
[22] B.P. Lee, Y. Liu, S. Konst, Novel Hydrogel Actuator Based on Biomimetic Chemistry. 2014 MRS Spring Meet, 2014.
[23] B.P. Lee, M. Lin, A. Narkar, S. Konst, R. Wilharm, Modulating the movement of hydrogel actuator based on catechol-iron ion coordination chemistry, Sens. Actuators B Chem. 206 (2015) 456–462, http://dx.doi.org/10.1016/j.snb.2014.09.089.
[24] A.B. Baker, D.F. Wass, R.S. Trask, Novel multi-stage three-dimensional deployment employing ionoprinting of hydrogel actuators, MRS Adv (2016) 1–6, http://dx.doi.org/10.1557/adv.2016.361.
[25] A.B. Baker, D.F. Wass, R.S. Trask, 4D sequential actuation: combining ionoprinting and redox chemistry in hydrogels, Smart Mater. Struct. 25 (2016) 10LT02, http://dx.doi.org/10.1088/0964-1726/25/10/10lt02.
[26] D. Morales, I. Podolsky, R. Mailen, T. Shay, M. Dickey, O. Velev, Ionoprinted multi-responsive hydrogel actuators, Micromachines 7 (2016) 98, http://dx.doi.org/10.3390/mi7060098.
[27] A.B. Baker, D.F. Wass, R.S. Trask, Bio-inspired reversible crosslinking, using chelating polymers and metal ion binding, for use as soft actuation and selective growth, in: Proc. 20th Int. Conf. Compos. Mater., Copenhagen, 2015.
[28] J. Na, A.A. Evans, J. Bae, M.C. Chiappelli, C.D. Santangelo, R.J. Lang, et al., Programming reversibly self-folding origami with micropatterned photo-crosslinkable polymer trilayers, Adv. Mater. 27 (2015) 79–85, http://dx.doi.org/10.1002/adma.201403510.

Biographies

Anna Baker She obtained her Ph.D. in Advanced Composites from the University of Bristol in 2017. And is currently a research assistant in Mechanical Engineering at the University of Bath. Her research interests are in actuating hydrogels and 4D printing.

Duncan Wass He obtained his Ph.D. in Chemistry from the Imperial College, London in 1998. And is currently Professor of Catalysis at the University of Bristol. His research interests are in the area of homogeneous catalysis and organometallic chemistry.

Richard Trask He obtained his Ph.D. in Composite Engineering from the University of Southampton in 2004. And is currently Professor of Advanced Materials at the University of Bath. His research interests are in the development of biologically inspired 3D and 4D multifunctional materials.